Coarse-Grained Simulation of the Adsorption of Water on Au (111) Surfaces Using a Modified Stillinger–Weber Potential

Journal:	*ACS Omega*
Manuscript ID	ao-2020-04071s.R2
Manuscript Type:	Article
Date Submitted by the Author:	n/a
Complete List of Authors:	Ripani, Giorgio; Università degli Studi di Roma Tor Vergata Macroarea di Scienze Matematiche Fisiche e Naturali, Scienze e tecnologie chimiche Flachmüller, Alexander; Universitat Konstanz, Theoretical Chemistry Peter, Christine; Universitat Konstanz, Theoretical Chemistry Palleschi, Antonio; University of Rome Tor Vergata, Scienze e Tecnologie Chimiche

SCHOLARONE™
Manuscripts

Coarse-Grained Simulation of the Adsorption of Water on Au (111) Surfaces Using a Modified Stillinger-Weber Potential

Giorgio Ripani [a], *Alexander Flachmüller* [b], *Christine Peter* [b*], *Antonio Palleschi* [a*]

[a] Department of Chemical Science and Technologies, University of Rome "Tor Vergata",

Via della Ricerca Scientifica, 00133 Rome, Italy

[b] Theoretical Chemistry , University of Konstanz , 78547 Konstanz , Baden-Württemberg ,

Germany

Corresponding Authors

* antonio.palleschi@uniroma2.it. *christine.peter@uni-konstanz.de

ABSTRACT. For reproducing the behavior of water molecules adsorbed on gold surfaces

in terms of density of both bulk and interfacial water and in terms of structuring of water on

top of gold atoms, the implementation of a multibody potential is necessary, thus the

Stillinger-Weber potential was tested. The goal is using a single non bonded potential for

coarse grained models, without the usage of explicit charges. In order to modify the

angular part of the Stillinger-Weber potential from a single cosine to a piecewise function

accounting for multiple equilibrium angles, employed for Au-Au-Au and Au-Au-water

triplets, it is necessary to create a version of the simulation package LAMMPS that

supports assignment of multiple favored angles. This novel approach is able to reproduce

the data obtained by quantum mechanical calculation and density profiles of both bulk and

adsorbed water molecules obtained by classical polarizable force fields.

1
2
3
4
5
6
7
8
9
10
11
12
13
14
15
16
17
18
19
20
21
22
23
24
25
26
27
28
29
30
31
32
33
34
35
36
37
38
39
40
41
42
43
44
45
46
47
48
49
50
51
52
53
54
55
56
57
58
59
60

KEYWORDS. Interface Force Field, Stillinger-Weber Potential, Coarse Grained Model,

Molecular Dynamics, Molinero-Water, Au Surface.

1. INTRODUCTION

In the last years, in nanoscience, the use of functionalized nanoparticles with biomolecules

has gained a lot of interest, with applications in drug delivery[1], theranostic[2], heterogeneous

catalysis[3], and clinic[4] and environmental[5] analysis. The functionalization is possible by

using covalently bonded molecules on Au surfaces by means of thiol groups. Non covalent

passivation is also used in water media to promote ligand exchange and to control the

nucleation-growth of nanoparticles[6]. With the aim of studying these systems with classical

molecular dynamics simulations, traditional force fields using exclusively two-body

potentials for the non-bonded interactions are no longer effective. An important example is

the simple adsorption of water on Au-(111) surface. Density Functional Theory (DFT)

calculations state that a single water molecule has to be on top, forming an angle of 90°

with two Au surface atoms and that hydrogen atoms do not have to point directly to the Au

3

surface[7]. These results cannot be reproduced by using only two body terms, even if we

are talking about water models at full atomistic resolution (including electrostatics). In fact,

calculations performed using a non-bonded attractive-repulsive two-body term for the

interaction of a single water molecule with a Face Centered Cubic (FCC) Au-(111) surface

will give rise to a large free-energy minimum on the "hollow" site (due to the contribution

from interactions with three surface atoms).

To overcome this problem a multibody potential becomes necessary and the three-body

Stillinger-Weber Potential (SWP) can be successfully used. SWP parameters for water

molecules in bulk[8], polyethylene[9], and organic solutes[10] in water are already present in the

literature. In the latter case the authors were able to reproduce the Potential of Mean

Force (PMF) of a methane dimer in water, establishing a basis for a CG force-field for

aqueous soft matter systems based only on non-bonded interaction without electrostatic

contributions. Other examples of efficient usage of the SWP are the original works on

Silicon[11], Gallium[12], tetrahedral Carbon[13], and other elements in cubic lattice[14].

Furthermore other CG applications with SWP exist for Calcite/Water nucleation-growth

mechanisms[15]. An implementation of three-body interactions, coupled with a polarizability

4

term in the two-body function, has been successfully used in classical molecular dynamics

simulations, in full atomistic representation, for the adsorption of water on Au surfaces[16].

Full atomistic models using electrostatic interactions alongside a fully parametrized three

body term for the physisorption or chemisorption of water on noble metal 111 surfaces are

reported by Steinmann et al.[17] and Clabaut et al.[18]

As far as we know, a simulation model for the adsorption of water on a Au surface using a

CG approach and without any explicit polarizability and/or electrostatic term does not exist

so far.

In this paper, we searched for an accurate description of the interaction between water

molecules represented by the Molinero water (mW) model[8] and an FCC Au-(111) surface,

parameterizing Au and water two- and three-body interactions in a modified version of the

SWP for CG molecular dynamics simulations.

The SWP functional form (eq. 1) is explicitly separable in two parts: an attractive-repulsive

term for the two-body interaction (eq. 2) and a purely repulsive three-body angular

dependence (eq. 3).

$$V_{SW}(r^N) = \sum_i \sum_{j>i} \varphi_2(r_{ij}) + \sum_i \sum_{j \neq i} \sum_{k>j} \varphi_3(r_{ij}, r_{ik}, \cos \theta_{jik}) \qquad (1)$$

5

$$\varphi_2(r_{ij}) = \begin{cases} A_{ij}\varepsilon_{ij}\left[B_{ij}\left(\frac{\sigma_{ij}}{r_{ij}}\right)^4 - 1\right]\exp\left(\frac{1}{\frac{r_{ij}}{\sigma_{ij}} - a_{ij}}\right), & \frac{r_{ij}}{\sigma_{ij}} < a_{ij} \\ \\ 0, & \frac{r_{ij}}{\sigma_{ij}} \geq a_{ij} \end{cases} \tag{2}$$

$$\varphi_3(r_{ij}, r_{ik}, \cos\theta_{ijk}) = \begin{cases} \lambda_{ijk}\varepsilon_{ijk}(\cos\theta_{ijk} - \cos\theta_0)^2\exp\left(\frac{\gamma_{ij}}{\frac{r_{ij}}{\sigma_{ij}} - a_{ij}} + \frac{\gamma_{ik}}{\frac{r_{ik}}{\sigma_{ik}} - a_{ik}}\right), & \frac{r_{il}}{\sigma_{il}} < a_{il} \\ \\ 0, & \frac{r_{il}}{\sigma_{il}} \geq a_{il} \end{cases} \tag{3}$$

Here A_{ij} and λ_{ijk} are the strengths of the two-body and three-body interactions and

alongside B_{ij}, σ_{ik}, a_{ij}, $\cos\theta_0$, γ_{ij} and ε_{ijk} represent the full set of parameters to completely

describe the SWP[11]: $\varepsilon_{ij} = \varepsilon_{ijj} = \varepsilon_{jii}$ according to LAMMPS definition.

In particular, for the two-body function (φ_2), it is possible to optimize the parameters in

order to reproduce the force constant, energy minimum and equilibrium distance, matching

the 0th, 1st and 2nd derivatives of the potential (eq.s 4), calculated at the equilibrium value

$(r = r_e)$.

$$\begin{cases} \left(\frac{\partial\varphi_2}{\partial r}\right)_{r_e} = 0 \rightarrow B\left(\frac{r_e}{\sigma}, a\right) = \dfrac{\left(\frac{r_e}{\sigma}\right)^4}{4\frac{\sigma}{r_e}\left(\frac{r_e}{\sigma} - a\right)^2 + 1} \\ \\ \varphi_2(r_e) = -\varepsilon \rightarrow A\left(\frac{r_e}{\sigma}, a\right) = \dfrac{\exp\left(\frac{1}{\frac{r_e}{a} - \frac{r_e}{\sigma}}\right)}{1 - \left(\frac{\sigma}{r_e}\right)^4 B\left(\frac{r_e}{\sigma}, a\right)} \\ \\ \left(\frac{\partial^2\varphi_2}{\partial r^2}\right)_{r_e} = k_f\left(\frac{r_e}{\sigma}, a\right) \end{cases} \tag{4}$$

6

With this approach the large number of parameters in the SWP can be reduced to only two

quantities, namely $\frac{r_e}{\sigma}$ and a.

2. METHODS

All the simulations have been performed using the simulation package LAMMPS[19] with a 5 fs

time step in the isothermal-isobaric (NPT) ensemble with a semi-isotropic pressure coupling.

Temperature and pressure were controlled by a Nosè-Hoover[20] thermostat and barostat using 100

ps, and 1 ns dumping constants, for temperature and pressure, respectively. The equilibrium

external pressures were 0, 0 and 1 atm for X, Y and Z, respectively, where Z is the axis normal to

the Au surface. The simulations were performed by using a box (5x5x9 nm^3) containing a slab of

2880 Au atoms (FCC) and 5785 water molecules and applying the periodic boundary conditions.

A piecewise function for the angular dependence of the SWP has been implemented in C++ as a

new pair style (link for LAMMPS downloadable input files and for the modified code :

https://github.com/gripani/XXX and https://github.com/gripani/YYY). Analysis of the simulations

have been performed by means of homemade programs.

3. RESULTS AND DISCUSSION

The parameters for the water-Au pair have been refined to reproduce the *a posteriori*

feature (mass density) of GolP-CHARMM polarizable Force Field[21].

The parameters for the Au bulk concerning the two-body part only have been obtained

starting from the cohesive energy ($E_C = \varepsilon$) , lattice parameter ($a_{Br} = r_e\sqrt{2}$) and bulk

modulus ($\mathcal{B} = \frac{2r_e^2}{3V_0}k_f$) already existing in literature[22].

7

Table 1. Optimized two-body SWP parameters for all the possible pairs in the system.

i	j	r_e (Å)	σ (Å)	a	A	B
mW	mW	2.685	2.393	1.800	7.04955628	0.60222
Au	Au	2.951	2.045	2.053	1.76300000	2.223000
mW	Au	3.000	2.250	2.150	5.10293601	1.053210

The three-body function (φ_3) depends on λ, γ, and $\cos\theta_0$. For the gamma value we

have used the already parametrized value, $\gamma = 1.2$[11], for all the possible triplets in the

system. According to Molinero, the tetrahedraility of bulk water is provided by $\cos\theta_0$

$= -1/3$ and $\lambda = 23.15$[8]. Concerning the Au FCC lattice in the bulk phase, it is not possible

to reproduce the three-body energy using a single value of equilibrium angle[14]. The same

issue, with more critical aspects, appears in the case of the mW-Au-Au triplet as well.

Indeed, one adsorbed water and its nearest neighbor Au atom, for the FCC lattice,

form an angle of 90 degrees with an Au atom of the first layer and an angle of 144.7

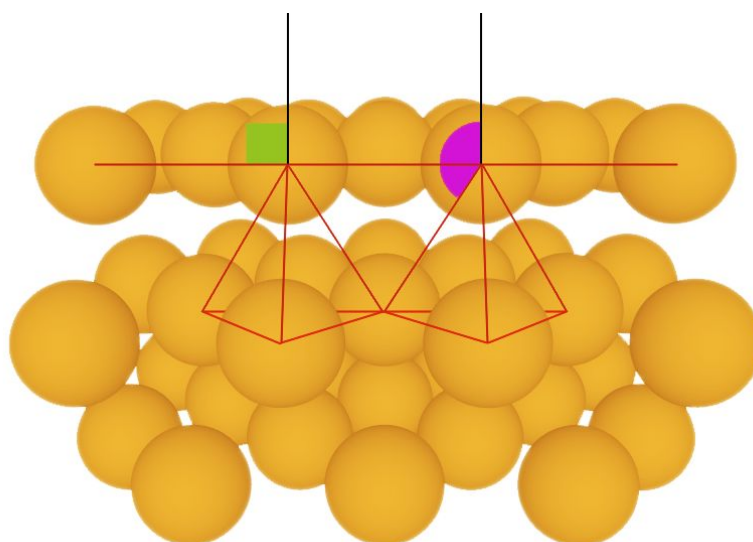degrees with a nearest neighbor Au of the second layer. (Fig. 1).

1
2
3
4
5
6
7
8
9
10
11
12
13
14
15
16
17
18
19
20
21
22
23
24
25
26
27
28
29
30
31
32
33
34
35
36
37
38
39
40
41
42
43
44
45
46
47
48
49
50
51
52
53
54
55
56
57
58
59
60

Figure 1. Schematic representation of the two different angles formed by the normal to the Au surface and two adjacent Au atoms, connected by red lines (corresponding to the Au-Au equilibrium distance). The 90 degrees angle is shown in light green and the 144.7 degrees angle is shown in violet.

The functional form of the piecewise function (eq. 5) concerning N different equilibrium

angles is the following (x_n^{min} and x_n^{max} are the limiting values of the n-th piece interval):

$$g(\cos\theta) = \left\{ g_n^0 + (-1)^{n+1}(\cos\theta - \cos\theta_n^e)^2 ; \; x_n^{min} \leq \cos\theta < x_n^{max} \right\}; n \in [1, 2N-1] \qquad (5)$$

In Table 2, the parameters of the piecewise function for an FCC lattice are reported.

The same g function with modified parameters (reported in Table 3) can be also used to

describe the behavior of water molecules interacting with the Au atoms, assuring the

preferential top site geometry.

9

Table 2. Parameters for the piecewise function associated with the Au-Au-Au triplet (FCC)

n	x_n^{min}	x_n^{max}	$\cos\theta_n^e$	g_n^0
1	-1	$-7/8$	-1	0
2	$-7/8$	$-5/8$	$-3/4$	$1/32$
3	$-5/8$	$-3/8$	$-1/2$	0
4	$-3/8$	$-1/8$	$-1/4$	$1/32$
5	$-1/8$	$1/8$	0	0
6	$1/8$	$3/8$	$1/4$	$1/32$
7	$3/8$	1	$1/2$	0

Table 3. Parameters for the piecewise function associated with the mW-Au-Au triplet

n	x_n^{min}	x_n^{max}	$\cos\theta_n^e$	g_n^0
1	-1	$-\dfrac{\sqrt{3/2}}{2}$	$-\sqrt{2/3}$	0
2	$-\dfrac{\sqrt{3/2}}{2}$	$-\dfrac{1}{2\sqrt{6}}$	$-\dfrac{1}{\sqrt{6}}$	$\dfrac{1}{12}$
3	$-\dfrac{1}{2\sqrt{6}}$	1	0	0

The value g_n^0 ensures continuity and derivability to the function that has to be evaluated numerically.

In order to implement the modified angular dependence for the multi-angle approach, we defined a new pairstyle in the LAMMPS source code (SWPmod).

Specifically the pairwise function $g(\cos\theta)$ (eq. 5) goes in place of $(\cos\theta_{ijk} - \cos\theta_0)^2$ in the three-body function (eq. 3).

Due to technical reasons we have introduced in our code a switch parameter, with the role of choosing which piecewise function is necessary for which triplet (alongside the full set of parameters n, x_n^{min}, x_n^{max}, $\cos\theta_n^e$, g_n^0). In this way, the approach can be easily extended to other molecular systems. In particular, if $switch = 0$ no piecewise function will be used (single angle harmonic cosine function); if $switch = 1$, the two angles piecewise function will be used for the mW, Au, Au triplet, as reported in Table 2; if $switch = 2$ the four angles piecewise function will be used (for bulk Au as reported in Table 1).

It is noteworthy that it is possible to realize a fine tuning of the correct top site configuration by changing the strength of the repulsive three-body term (λ) for the mW-Au-Au triplet. Fig. 2 (top) shows the average orientation of water molecules respect to the Au surface sites. The figure nicely illustrates how it is possible to shift the equilibrium configuration of the adsorbed water molecules from the hollow to the top sites, performing NPT simulations with different λ values.

Table 4. Three-body SWPmod parameters used in all the simulations.

i	j	k	ε $(kcal/mol)$	λ	$\cos\theta_0$	γ	$switch$

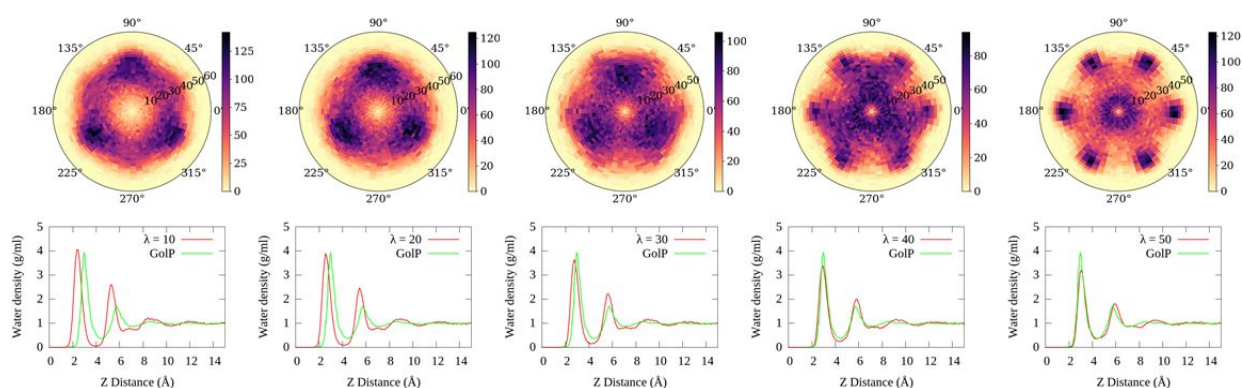| mW	mW	mW	6.189	23.15	-1/3	1.2	0
Au	Au	mW	2.000	10-50	/	1.2	1
Au	Au	Au	73.94	10.00	/	1.2	2

Figure 2. Top) Water densities at different lambda values for the mW, Au, Au triplet (10, 20, 30, 40, 50, from left to right). The polar plots report the water density (see color code on the right) as a function of polar and azimuthal angles referred to the vector connecting a single Au atom to the first neighbor water molecule, averaged on all the Au atoms of the surface. The water adsorption preferences of the angles on the azimuthal axes refer to about 20° for hollow sites and 0° and about 40° for top sites (central and next Au atoms). Bottom) Time averaged Z density of water (g/ml) of NPT simulations (in red) and GolP reference (in green) *vs* the distance (Å) of water molecules from the Au surface.

From the water density in z-direction (i.e. normal to the surface) the PMF of the adsorption of the

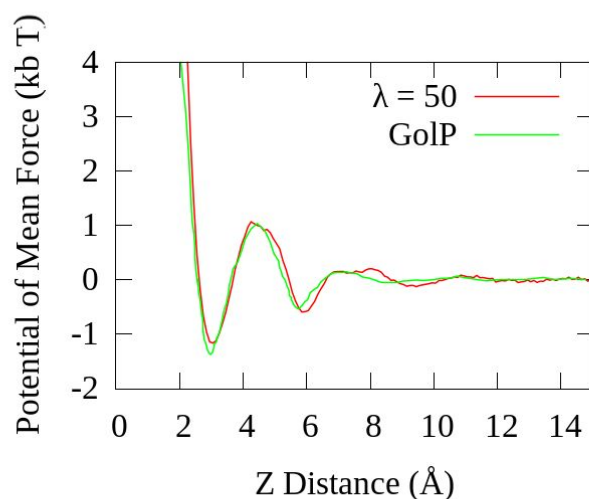water molecules on the Au surface can be obtained (eq. 6).

Figure 3. Potential of Mean Force obtained by density profile (λ=50 in red) and GolP reference (in green). The two minima correspond to the first (3.0 Å) and second (4.5 Å) layers of adsorbed mW.

The two minima correspond to the first and second layer of adsorbed molecules, from which it is possible to estimate both equilibrium (eq. 7) and kinetic (eq. 8) constants of the exchange process between the two layers (corresponding to the first and second minima of Figure 3 in the case λ=50).

$$\beta W(Z) = -\log\left(\frac{\rho(Z)}{\rho(\infty)}\right) \tag{6}$$

$$K_{eq} = \exp\left(-\beta\Delta W^0\right) = 1.82 \tag{7}$$

$$k = (\beta h)^{-1}\exp\left(-\beta\Delta W^\dagger\right) = 1.14\ ps^{-1} \tag{8}$$

ΔW^0 is the difference between the values of the PMF of the first and the second minimum and $\Delta W^\dagger$ is the difference between the value of the PMF calculated at the first maximum and the value of the PMF calculated at the first minimum. In Eyring equation (eq. 8) the transmission coefficient is set equal to 1, as it is usually assumed for transport processes.

4. CONCLUSIONS

In conclusion, with the support of a multibody potential we were able to reproduce the correct configuration of adsorbed water molecules on Au-(111) surface and the water density profile as obtained by GolP-CHARMM force field. The model is also able to describe the first and second layer of adsorbed water molecules. The advantages of this approach are the absence of explicit partial charges so that it does not need any electrostatic contribution on the energy and the reduced number of simulated particles with the CG approach. In contrast the GolP-CHARMM force field makes use of explicit dummy charges bound to Au atoms and is fully atomistic. Finally, the versatility and general form of the three-body part of the Stillinger-Weber potential allows a possible extension of the proposed approach to other molecular systems.

AUTHORS INFORMATION

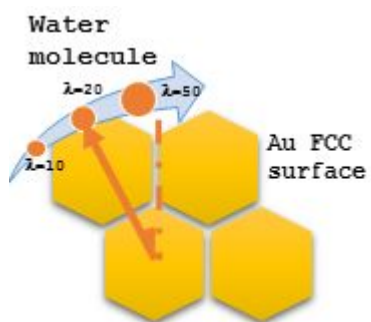* antonio.palleschi@uniroma2.it. *christine.peter@uni-konstanz.de

REFERENCES

(1) Ferris, D. P. ; Lu J. ; Gothard, C. ; Yanes, R. ; Coutney, R. T ; Olsen, J.C ; Stoddart, J. F ; Tamanoi, F. and Zink, J. I. Synthesis of biomolecule-modified mesoporous silica

14

nanoparticles for targeted hydrophobic drug delivery to cancer cells. *Small* **2011**, 7(13),

1816-1826

(2) Biscaglia, F; Ripani, G.; Rajendran, S; Benna, C.; Mocellin, S.; Bocchinfuso, G.; Meneghetti M.; Palleschi, A. and Gobbo, M. Gold Nanoparticle Aggregates functionalized

with cuclic RGD paptides for targeting and imaging of colorectal cancer cells. *ACS Appl.*

Nano Mater. **2019**, 2, 10, 6436-6444

(3) Roy, S.; Pericas, M.A; Functionalized nanoparticles as catalysts for enantioselective processes. *Org. Biomol. Chem.* **2009**, 7, 2669-2677

(4) Anselmo, A. C. and Mitragotri S. Nanoparticles in the clinic, *Bioeng Transl Med.* **2016** 1(1): 10–29

(5) Kolataj, K; Krajcewski, J. and Kudelski, A. Plasmonic nanoparticles for environmental analysis Environ Chem Lett **2020**, 18, 529-242

(6) Hughes, Z. E.; Walsh, T.R. Non-covalent adsorption of amino acid analogues on noble-metal nanoparticles: influence of edges and vertices. *Phys. Chem. Chem. Phys.* **2016**, 26, 18

(7) Berg, A.; Peter, C.; Johnston, K. Evaluation and Optimization of Interface Force Fields for Water on Gold Surfaces. *J. Chem. Theory Comput.* **2017**, 13, 11, 5610-5623

(8) Molinero, V.; Moore, E. B.. Water modeled as an intermediate element between carbon and silicon. *J. Phys. Chem. B* **2009**, 113, 13, 4008-16

(9) Raubenolt, B.; Gyawali, G.; Tang, W.; Wong, K. S.; Rick, S.W. Coarse-Grained Simulations of Aqueous Thermoresponsive Polyethers, *Polymers* **2018**, 10, 475

(10) Molinero, V.; Song, B. Thermodynamic and structural signatures of water-driven methane-methane attraction in coarse-grained mW water. *J. Chem. Phys.,* **2013**, 139, 054511

(11) Stillinger, F. H.; Weber. T. A. Computer simulation of local order in condensed phases of silicon. *Physical Review B,* **1985**, 31, 8

(12) Bere, A.; Serra, A. On the atomic structures, mobility and interactions of extended defects in GaN: dislocations, tilt and twin boundaries. *Philosophical Magazine A,* **2006**, 86, 15,

2159-2192

15

(13) Barnard, A. S.; Russo, S.P. Development of an improved Stillinger-Weber potential for tetrahedral carbon using ab initio (Hartree-Fock and MP2) methods. *Molecular Physics* **2002**, 100, 10, 1517-1525

(14) Zhou, X. W.; Wadley, H.N.G. A potential for simulating the atomic assembly of cubic elements. *Comput. Mater. Science*, **2009**, 39, 2, 340-348

(15) King, M.; Pasler, S.; Peter, C.. Coarse-Grained Simulation of CaCO3Aggregation and Crystallization Made Possible by Nonbonded Three-BodyInteractions. *J.Phys.Chem.C* **2019**, 123, 3152−3160

(16) Siepmann I., J. , Sprik M. Influence of surface topology and electrostatic potential on water/electrodesystems *J. Chem. Phys.* **1995** 102, 511 (1995)

(17) Steinmann S. N., De Morais R. F., Gotz A. W., Fleurat-Lessard P., Ianuzzi M., Sautet P., Michel C. Force Field for Water over Pt(111): Development, Assessment, and Comparison *J. Chem. Theory Comput.* **2018**, 14, 6, 3238–3251

(18) Claubaut P., Fleurat-Lessard P., Michel C. Steinmann S. N. Ten Facets, One Force Field: The GAL19 Force Field for Water–Noble Metal Interfaces *J. Chem. Theory Comput.* **2020**, 16, 7, 4565–4578

(19) Plimpton, S. Fast Parallel Algorithms for Short-Range Molecular Dynamics, *J Comp Phys*, **1995** , 117, 1-19

(20) Evans, B. ; Holian, B. L. The Nose-Hoover thermostat *J. Chem. Phys.* **1985** 83, 4069

(21) Wright, L.B.; Rodger, P.M.; Corni, S.; Walsh, T.R. GolP-CHARMM: First-Principles Based Force Fields for the Interaction of Proteins with Au(111) and Au(100). *J. Chem. Theory Comput.* **2013**, 9, 1616−1630

(22) Ambrosetti, A.; Silvestrelli, P.L. Cohesive properties of noble metals by van der Waals-corrected Density Functional Theory. *Phys. Rev. B*, **2016**, 94, 045124

FOR TABLE OF CONTENTS ONLY

1
2
3
4
5
6
7
8
9
10
11
12
13
14
15
16
17
18
19
20
21
22
23
24
25
26
27
28
29
30
31
32
33
34
35
36
37
38
39
40
41
42
43
44
45
46
47
48
49
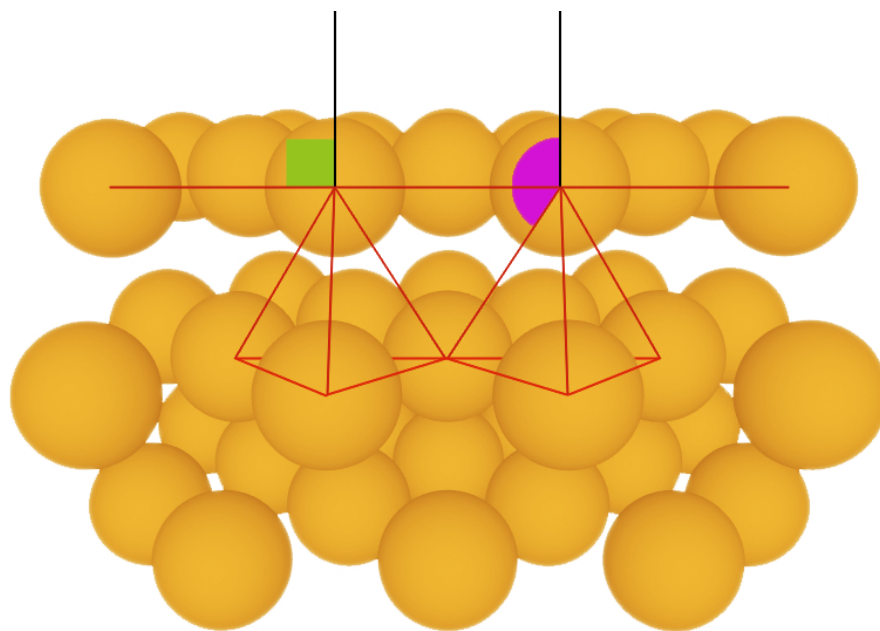50
51
52
53
54
55
56
57
58
59
60

Figure 1. Schematic representation of the two different angles formed by the normal to the Au surface and two adjacent Au atoms, connected by red lines (corresponding to the Au-Au equilibrium distance). The 90 degrees angle is shown in light green and the 144.7 degrees angle is shown in violet.
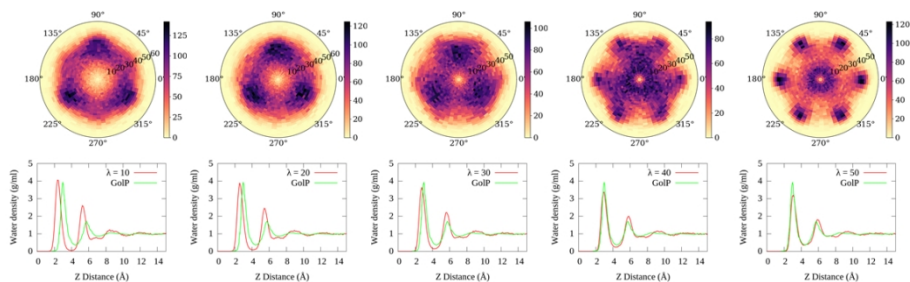
300x197mm (72 x 72 DPI)

Figure 2. Top) Water densities at different lambda values for the mW, Au, Au triplet (10, 20, 30, 40, 50, from left to right). The polar plots report the water density (see color code on the right) as a function of polar and azimuthal angles referred to the vector connecting a single Au atom to the first neighbor water molecule, averaged on all the Au atoms of the surface. The water adsorption preferences of the angles on the azimuthal axes refer to about 20° for hollow sites and 0° and about 40° for top sites (central and next Au atoms). Bottom) Time averaged Z density of water (g/ml) of NPT simulations (in red) and GoIP reference (in green) vs the distance (Å) of water molecules from the Au surface.
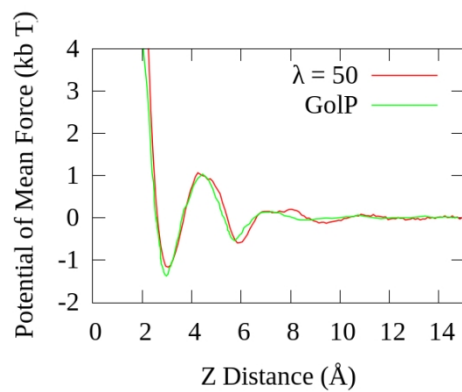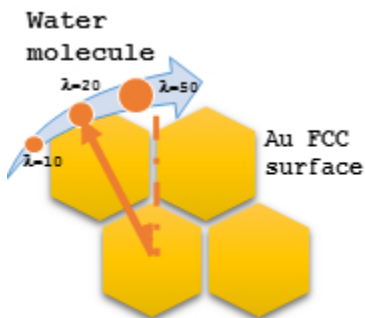
338x190mm (96 x 96 DPI)

1
2
3
4
5
6
7
8
9
10
11
12
13
14
15
16
17
18
19
20
21
22
23
24
25
26
27
28
29
30
31
32
33
34
35
36
37
38
39
40
41
42
43
44
45
46
47
48
49
50
51
52
53
54
55
56
57
58
59
60

Figure 3. Potential of Mean Force obtained by density profile (λ=50 in red) and GolP reference (in green). The two minima correspond to the first (3.0 Å) and second (4.5 Å) layers of adsorbed mW.

338x190mm (96 x 96 DPI)

1
2
3
4
5
6
7
8
9
10
11
12
13
14
15
16
17
18
19
20
21
22
23
24
25
26
27
28
29
30
31
32
33
34
35
36
37
38
39
40
41
42
43
44
45
46
47
48
49
50
51
52
53
54
55
56
57
58
59
60

50x50mm (96 x 96 DPI)